FT-IR Study of the Perpendicular Bands of 1,3,5-Triazine I:* The ν_7 and ν_9 Bands of $^{12}C_3{}^{14}N_3H_3$, $^{13}C_3{}^{14}N_3H_3$, $^{12}C_3{}^{15}N_3H_3$ and the Difference Band $\nu_9-\nu_{14}$ of $^{12}C_3{}^{14}N_3H_3$

M. Pfeffer, W. Bodenmüller, and A. Ruoff

Sektion Schwingungsspektroskopie, Universität Ulm, Albert-Einstein-Allee 11, D-89069 Ulm

Z. Naturforsch. **53a**, 670–678 (1998); received March 31, 1998

Dedicated to Dr. Georges Graner on the occasion of his 65th birthday

The analysis of the high resolution FT-IR spectra of the perpendicular bands $\nu_7(E')$ at about 1550 cm^{-1} and $\nu_9(E')$ at about 1170 cm^{-1} of the isotopomers $^{12}C_3{}^{14}N_3H_3$, $^{13}C_3{}^{14}N_3H_3$, and $^{12}C_3{}^{15}N_3H_3$ is given. Both bands proved to be free from accidental resonances. The molecular constants of the state $\boldsymbol{v}_7 = 1$ and $\boldsymbol{v}_9 = 1$ of the isotopomers under consideration are listed. The weak difference band $\nu_9-\nu_{14}(E'' \rightarrow E')$ of $^{12}C_3{}^{14}N_3H_3$ was recorded and analyzed, using the molecular constants of $\boldsymbol{v}_9 = 1$ [this work] and $\boldsymbol{v}_{14} = 1$ [of 1995]. This analysis proves the quality of the molecular constants of the fundamental ν_{14} which is IR-inactive.

Key words: High Resolution FT-IR Spectroscopy; 1,3,5-Triazine, Perpendicular Band; Difference Band.

1. Introduction

1,3,5-Triazine, $C_3N_3H_3$ (henceforth abbreviated as triazine), is a planar symmetric top molecule belonging in the molecular symmetry group $D_{3h}(M)$, under which μ_e is forbidden. Therefore, high resolution IR- and/or Raman spectroscopy of triazine in its gaseous phase is the appropriate tool for getting informations on the molecular structure and potential of this molecule.

Amongst the 14 normal vibrations of triazine seven are IR-active: the two parallel bands ν_{11} and ν_{12} (A_2''), and the five perpendicular bands ν_6, ν_7, ν_8, ν_9 and $\nu_{10}(E')$.

The analysis of the high resolution FT-IR spectra of the fundamental bands ν_{11} and ν_{12} of the isotopomers $^{12}C_3{}^{14}N_3H_3$, $^{13}C_3{}^{14}N_3H_3$, $^{12}C_3{}^{15}N_3H_3$, $^{13}C_3{}^{15}N_3H_3$ and $^{12}C_3{}^{14}N_3D_3$ by our group [1–3] yielded among other things the ground state constants of all molecules considered and an r_0- and r_s-structure of triazine [4].

In the present paper we report on the analysis of high resolution FT-IR spectra ** of the perpendicular fundamentals ν_7 (at about 1550 cm^{-1}) and ν_9 (at about 1170 cm^{-1}) of the isotopomers $^{12}C_3{}^{14}N_3H_3$, $^{13}C_3{}^{14}N_3H_3$ and $^{12}C_3{}^{15}N_3H_3$ and of the difference band $\nu_9-\nu_{14}$ of $^{12}C_3{}^{14}N_3H_3$.

2. Experimental

The sample of $^{12}C_3{}^{14}N_3H_3$ with a purity of 98% has been obtained from Merck-Schuchardt. Since no impurities could be detected in the IR spectra, the material was used without further purification. The $^{13}C_3{}^{14}N_3H_3$ and $^{12}C_3{}^{15}N_3H_3$ isotopomers were synthesized in a two step method with $K^{13}CN/KC^{15}N$ as starting material [3]. The raw products were purified by sublimation. The overall-yield was about 69%.

All spectra have been recorded at room temperature with the Bruker IFS 120 HR instruments at the University of Gießen and at the University of Oulu, respectively. Stainless steel cells with CsI and KBr windows, respectively, have been employed. The maximum optical path difference was between 370 cm and 542 cm. A Ge:Cu detector was used operating at 4 K. All other experimental details are summarized in Table 1.

Boxcar apodization has been applied to the interferograms. Calibration has been done by comparison with CO_2 and H_2O lines, the wavenumbers of which were taken from [5].

* Partly from the Thesis of W. Bodenmüller.

** Lists of observed and calculated wavenumbers as well as the correlation matrices have been deposited in the "Sektion Spektren- und Strukturdokumentation", Universität Ulm, 89069 Ulm (Dr. J. Vogt).

Reprint requests to Prof. A. Ruoff; Fax: +49-731-5023112.

0932-0784 / 98 / 0800-0670 $ 06.00 © – Verlag der Zeitschrift für Naturforschung, D-72027 Tübingen

Table 1. Experimental details of the IR-spectra of the isotopomers of triazine.

Isotopomer	Band	Range [cm^{-1}]	Pressure [mbar]	Scans	Resolution [cm^{-1}]	Cell length [m]
$^{12}C_3{}^{14}N_3H_3$	ν_7	1525–1585	0.5	210	0.0021	0.3
	ν_9	1135–1210	2.46	375	0.0018	3.28
	$\nu_9 - \nu_{14}$	800–870	1.11/2.40	470/200	0.0021/0.0024	144/144
$^{12}C_3{}^{15}N_3H_3$	ν_7	1510–1570	0.12	300	0.0020	3.28
	ν_9	1210–1280	0.12	300	0.0020	3.28
$^{13}C_3{}^{14}N_3H_3$	ν_7	1490–1560	0.116	360	0.0020	3.28
	ν_9	1120–1190	1.51	300	0.0018	13.12

The absolute accuracy of the calibration lines was between $1 \cdot 10^{-3}$ cm^{-1} and $1 \cdot 10^{-4}$ cm^{-1}. The relative accuracy of the peakfinder evaluated lins of triazine is about $\pm 2 \cdot 10^{-4}$ cm^{-1}.

3. Theory

As is well known, a planar symmetric top molecular like triazine in its equilibrium configuration is characterized by the planarity relations [6]

$$B_e = 2C_e,$$
$$2D_J^e + 3D_{JK}^e + 4D_K^e = 0,$$
$$3H_J^e + 4H_{JK}^e + 5H_{KJ}^e + 6H_K^e = 0. \quad (1)$$

These relations hold also approximately for the ground state.

The energy expression employed comprises the usual diagonal elements of the rovibrational Hamiltonian up to $\hat{h}_4^\dagger$:

$$\begin{aligned} &E(v,J,K) = \\ &\nu_0 + B_v J(J+1) + (C_v - B_v)k^2 \\ &- D_J^v J^2(J+1)^2 - D_{JK}^v J(J+1)k^2 \\ &- D_K^v k^4 + H_J^v J^3(J+1)^3 \\ &+ H_{JK}^v J^2(J+1)^2 k^2 + H_{KJ}^v J(J+1)k^4 \\ &+ H_K^v k^6 - l_t k\left[2(C\zeta_t^z)_v - \eta_v^J J(J+1)\right. \\ &- \eta_v^K k^2 - \eta_v^{JJ} J^2(J+1)^2 \\ &\left. - \eta_v^{JK} J(J+1)k^2 - \eta_v^{KK} k^4\right]. \end{aligned} \quad (2)$$

Here ν_0 equals zero for the ground state, and the vibrational quantum number l equals zero for all nondegenerate states.

Only the off-diagonal elements of the $q_t^{(+)}$-resonance proved to be of importance in the present investigation. They have been used in the form [7]

$$\begin{aligned} &\left\langle v_t, l_t, J, k \middle| \hat{h}_{2,2}^\dagger + \hat{h}_{2,4}^\dagger \middle| v_t, l_t \pm 2, J, k \pm 2 \right\rangle = \\ &-1/4\left[q_t^{(+)} + q_t^{(+)J} J(J+1) + q_t^{(+)K} k^2\right] \\ &F(J,k)F(J,k+1)v(t,t) \\ &\text{with} \quad F(J,k) = \left[J(J+1) - k(k \pm 1)\right]^{1/2} \\ &\text{and} \quad v(t,t) = \left[(v_t \pm l_t + 2)(v_t \mp l_t)\right]^{1/2}, \end{aligned} \quad (3)$$

the Mills convention [8] being adopted.

The r_t-resonance has not to be taken into account because it is forbidden under $D_{3h}(M)$.

4. Spectra and Analysis

4.1. Ground State

The ground state constants for all isotopomers considered have been determined recently [3] from the parallel bands ν_{11} and ν_{12} by a GSCD-program. They are listed in Table 2.

4.2. The ν_7 Fundamental Band of $^{12}C_3{}^{14}N_3H_3$, $^{13}C_3{}^{14}N_3H_3$, and $^{12}C_3{}^{15}N_3H_3$

The most intense fundamental of triazine is the perpendicular band $\nu_7(E')$ at 1556 cm^{-1} ($^{12}C_3{}^{14}N_3H_3$), 1524 cm^{-1} ($^{13}C_3{}^{14}N_3H_3$) and 1542 cm^{-1} ($^{12}C_3{}^{15}N_3H_3$) (Figure 1).

Contrary to all other IR-active perpendicular bands of triazine, the ν_7 exhibits no PQR-structure: The positive value of ζ_7^z of about +0.47 prevents cluster-formation in the Q-branch region spreading out the Q-lines over a wide area.

As another result of the positive value of ζ_7^z, the essential $q_t^{(+)}$-resonance is very weakly pronounced in the ν_7 band. At the present resolution, this band proved to be free from accidental resonances, the nearest vibrational level being more than 30 cm^{-1} apart from ν_7^0.

The assignment was begun with a band contour analysis on the basis of the results of Daunt and Shurvell [9] from a medium resolution Raman spectrum of the perpendicular band ν_7. The band contour simulation enabled

Table 2. Ground state constants [cm^{-1}] of triazine isotopomers (numbers in parentheses are one standard deviation in units of the last significant digit). **: from planarity conditions.

	$^{12}C_3{}^{14}N_3H_3$	$^{13}C_3{}^{14}N_3H_3$	$^{12}C_3{}^{15}N_3H_3$	$^{13}C_3{}^{15}N_3H_3$	$^{12}C_3{}^{14}N_3D_3$
C_0^{**}	0.1074	0.1041	0.1037	0.1006	0.0969
B_0	0.21486152(10)	0.20819716(6)	0.20741116(8)	0.20119592(9)	0.19377014(83)
D_J^0	$5.3419(56) \cdot 10^{-08}$	$5.0191(29) \cdot 10^{-08}$	$5.0196(36) \cdot 10^{-08}$	$4.7131(39) \cdot 10^{-08}$	$3.96743(40) \cdot 10^{-08}$
D_{JK}^0	$-8.861(16) \cdot 10^{-08}$	$-8.3267(83) \cdot 10^{-08}$	$-8.330(10) \cdot 10^{-08}$	$-7.8178(91) \cdot 10^{-08}$	$-6.5400(12) \cdot 10^{-08}$
D_K^{0**}	$3.98 \cdot 10^{-08}$	$3.74 \cdot 10^{-08}$	$3.74 \cdot 10^{-08}$	$3.51 \cdot 10^{-08}$	$2.92 \cdot 10^{-08}$
H_J^0	$2.7(11) \cdot 10^{-14}$	$1.84(42) \cdot 10^{-14}$	$2.05(52) \cdot 10^{-14}$	$1.41(52) \cdot 10^{-14}$	$1.73(59) \cdot 10^{-14}$
H_{JK}^0	$-1.52(40) \cdot 10^{-13}$	$-8.9(15) \cdot 10^{-14}$	$-3.5(20) \cdot 10^{-14}$	$-9.9(15) \cdot 10^{-14}$	$-5.8(23) \cdot 10^{-14}$
H_{KJ}^0	$2.93(69) \cdot 10^{-13}$	$1.70(25) \cdot 10^{-13}$	$-3.5(35) \cdot 10^{-14}$	$2.21(23) \cdot 10^{-13}$	$1.26(48) \cdot 10^{-13}$
H_K^{0**}	$-1.6 \cdot 10^{-13}$	$-9.2 \cdot 10^{-14}$	$4.2 \cdot 10^{-14}$	$-1.2 \cdot 10^{-13}$	$-7.5 \cdot 10^{-14}$
σ	$88 \cdot 10^{-06}$	$119 \cdot 10^{-06}$	$85 \cdot 10^{-06}$	$120 \cdot 10^{-06}$	$197 \cdot 10^{-06}$
GSCD's	937	2535	1005	1562	5223

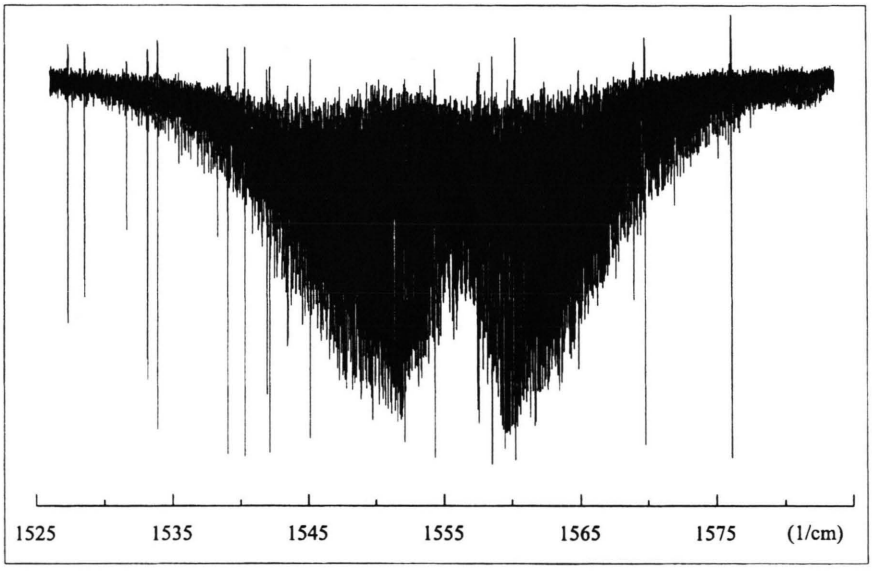

Fig. 1. Survey spectrum of the fundamental band $\nu_7(E')$ of $^{12}C_3{}^{14}N_3H_3$.

insights in the structure of the band showing cluster formations of the lines $^{\Delta K}\Delta K_{K\text{-}3n}(K\text{-}2n)$ (Fig. 2) in the ^{P}P- and ^{R}R-branches and allowed the location of the $^{R}Q_0$-subband (Fig. 3), which exhibits an intensity alternation of its J-lines caused by the spin statistics for $K = 0$ (Table 3).

With the aid of ground state combination differences (GSCD's) it was possible to assign 6215 lines with $-81 \le \Delta KK$ 83 and $-95 \le \Delta KJ \le 94$ of $^{12}C_3{}^{13}N_3H_3$, 10023 lines with $-90 \le \Delta KK \le 88$ and $-90 \le \Delta KJ \le 89$ of $^{13}C_3{}^{14}N_3H_3$ and 7085 lines with $-90 \le \Delta KK \le 84$ and $-90 \le \Delta KJ \le 89$ of $^{12}C_3{}^{15}N_3H_3$, and to establish the parameters of the excited state $v_7 = 1$ (Table 4) by using the least-squares fit program MILLI [10]. Only unblend-

Table 3. Spin weights of the rovibrational levels of all isotopomers of triazine considered.

Isotopomer	K	$\Gamma_{\|v\rangle}$		
		A_1', A_1''	A_2', A_2''	E', E''
$^{12}C_3{}^{14}N_3H_3$	0 (J even)	20	56	70
	0 (J odd)	56	20	70
	$3p \pm 1$	70	70	[20 + 56] + 70
	$3p$	[20 + 56]	[20 + 56]	70 + 70
$^{13}C_3{}^{14}N_3H_3$	0 (J even)	364	220	572
	0 (J odd)	220	364	572
	$3p \pm 1$	572	572	[364 + 220] + 572
	$3p$	[364 + 220]	[364 + 220]	572 + 572
$^{12}C_3{}^{15}N_3H_3$	0 (J even)	20	4	20
	0 (J odd)	4	20	20
	$3p \pm 1$	20	20	[20 + 4] + 20
	$3p$	[20 + 4]	[20 + 4]	20 + 20

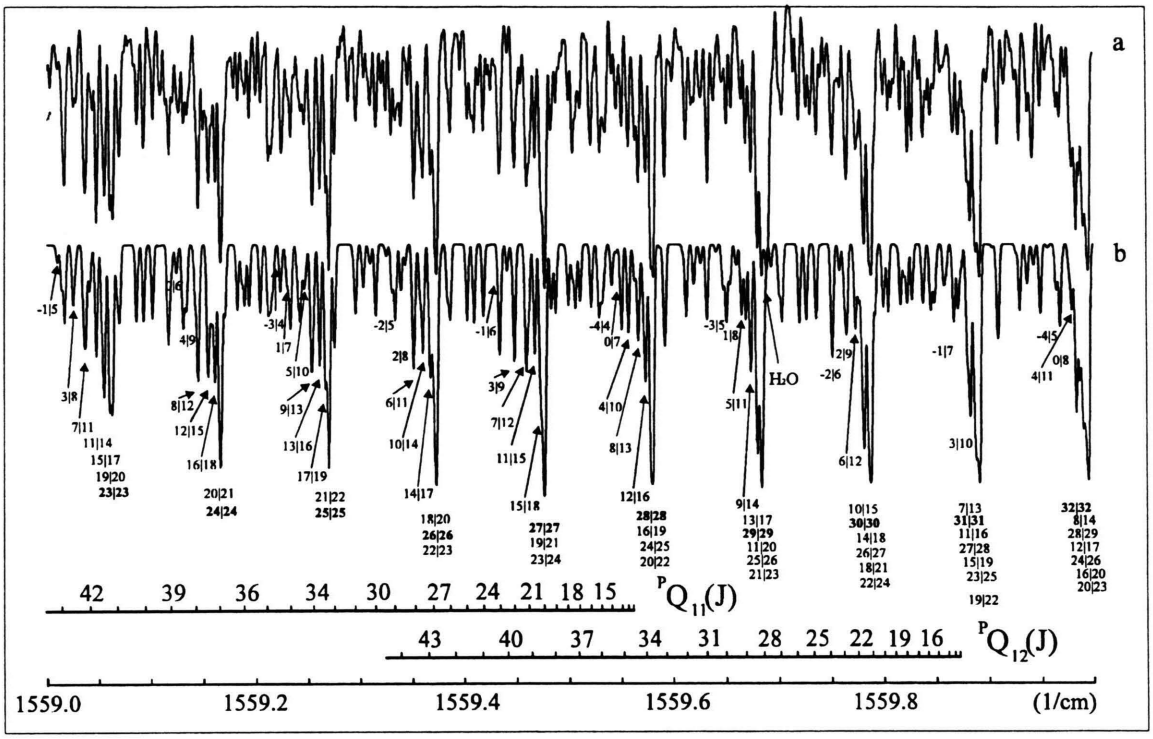

Fig. 2. Detail of the perpendicular band ν_7 of $^{12}C_3{}^{14}N_3H_3$. Some $^{R}R_K(J)$-, $^{P}R_K(J)$- and $^{P}Q_K(J)$-lines are marked. Bold numbers represents band headings. (a) Experimental spectrum. (b) Calculated spectrum.

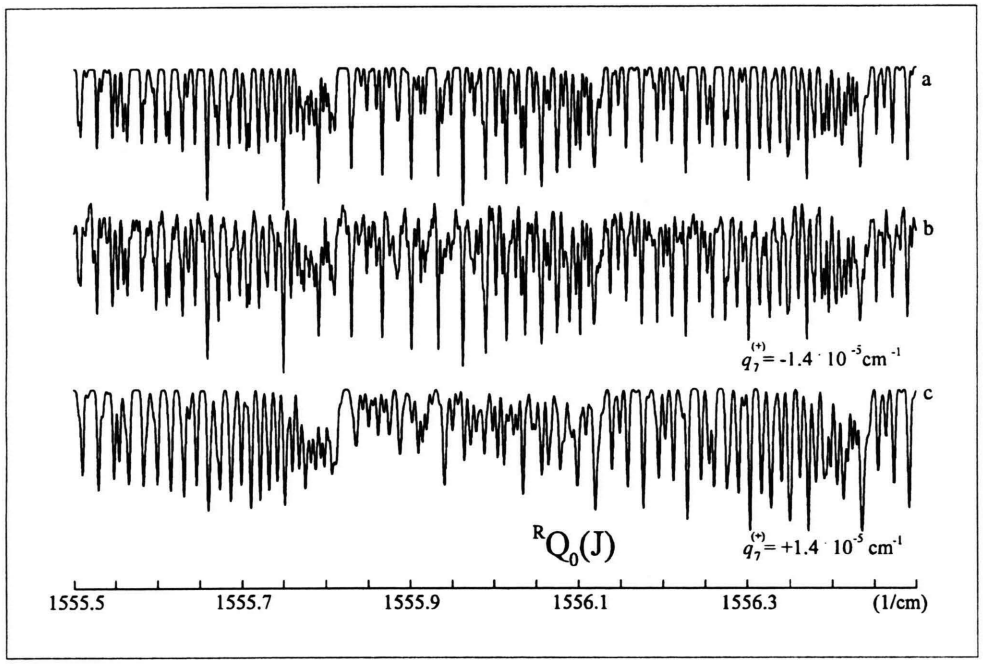

Fig. 3. Simulation of the $^{R}Q_0$-subband of the ν_7 band of $^{12}C_3{}^{14}N_3H_3$ for the determination of the $q_7^{(+)}$resonance. (a) Experimental spectrum. (b) Calculated spectrum ($q_7^{(+)}$ negative). (c) Calculated spectrum ($q_7^{(+)}$ positive).

Table 4. Molecular constants [cm^{-1}] of the ν_7 band of triazine isotopomers. (Numbers in parentheses are one standard deviation in units of the last significant digit). [a] Fixed values.

	$^{12}C_3{}^{14}N_3H_3$	$^{13}C_3{}^{14}N_3H_3$	$^{12}C_3{}^{15}N_3H_3$
ν_0	1556.338675(10)	1523.9991305(70)	1541.6637908(63)
$C'' - C'$	$2.15726(22) \cdot 10^{-4}$	$1.87896(14) \cdot 10^{-4}$	$2.040952(66) \cdot 10^{-4}$
$B'' - B'$	$3.093372(84) \cdot 10^{-4}$	$2.74860(12) \cdot 10^{-4}$	$2.706030(49) \cdot 10^{-4}$
$(C\zeta)'$	$5.018151(28) \cdot 10^{-2}$	$4.9765685(96) \cdot 10^{-2}$	$4.100121(10) \cdot 10^{-2}$
$D_J'' - D_J'$	$2.206(15) \cdot 10^{-10}$	$1.782(44) \cdot 10^{-10}$	$2.1447(77) \cdot 10^{-10}$
$D_{JK}'' - D_{JK}'$	$5.252(80) \cdot 10^{-10}$	$7.69(11) \cdot 10^{-10}$	$4.351(21) \cdot 10^{-10}$
$D_K'' - D_K'$	$-6.81(10) \cdot 10^{-10}$	$-7.08(10) \cdot 10^{-10}$	$-8.305(17) \cdot 10^{-10}$
η^J	$2.4116(38) \cdot 10^{-7}$	$3.01132(60) \cdot 10^{-7}$	$2.07596(59) \cdot 10^{-7}$
η^K	$-8.359(44) \cdot 10^{-8}$	$-1.54624(80) \cdot 10^{-7}$	$-3.561(66) \cdot 10^{-9}$
$H_J'' - H_J'$	0[a]	$-8.98(43) \cdot 10^{-15}$	
$H_{JK}'' - H_{JK}'$	0[a]	$-8.17(16) \cdot 10^{-14}$	
$H_{KJ}'' - H_{KJ}'$	$-5.2(17) \cdot 10^{-15}$	$2.789(23) \cdot 10^{-13}$	
$H_K'' - H_K'$	$7.8(18) \cdot 10^{-15}$	$-1.518(12) \cdot 10^{-13}$	
η^{JJ}	$2.19(61) \cdot 10^{-13}$		
η^{JK}	$-4.0(12) \cdot 10^{-13}$		
η^{KK}	$-2.06(88) \cdot 10^{-13}$		
$q_7^{(+)}$	$-1.4325(41) \cdot 10^{-5}$	$-8.602(37) \cdot 10^{-6}$	$-1.2951(22) \cdot 10^{-5}$
σ	$304 \cdot 10^{-6}$	$347 \cdot 10^{-6}$	$212 \cdot 10^{-6}$
number of lines	6215	10023	7085

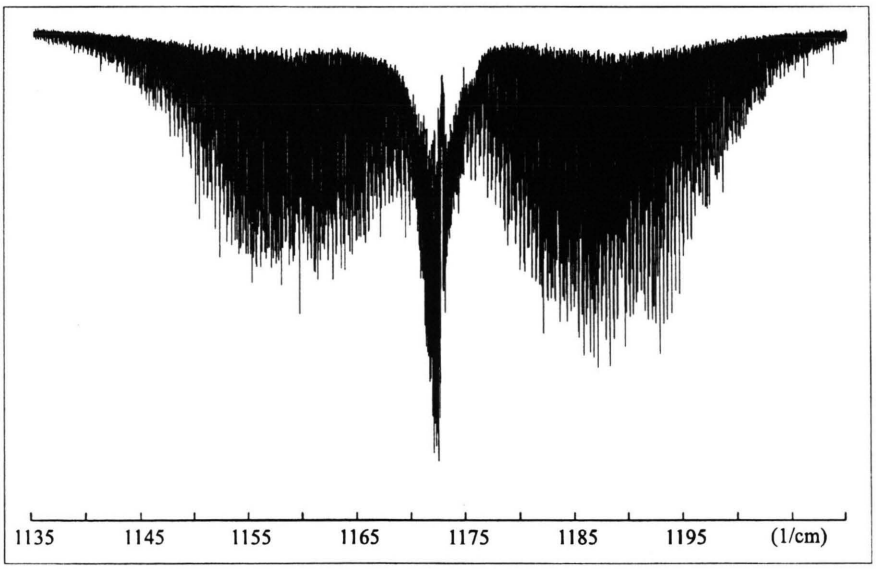

Fig. 4. Survey spectrum of the fundamental band $\nu_9(E')$ of $^{12}C_3{}^{14}N_3H_3$.

ed and equally weighted lines have been used throughout.

As can be seen, it was possible for $^{13}C_3{}^{14}N_3H_3$ to determine all fourth order parameters given in (2), in the case of $^{12}C_3{}^{14}N_3H_3$ it was only possible to determine some of them, while they remained undetermined for the $^{12}C_3{}^{15}N_3H_3$ isotopomer. In spite of this, the standard deviation of the fits was significantly lower for $^{12}C_3{}^{15}N_3H_3$, due to the higher resolution and the better signal-to-noise ratio of the spectrum of this isotopomer.

To include lines with low values of K into the fit it was necessary to introduce a small $q_7^{(+)}$-interaction term as given in (3), neglecting the $\hat{h}_{2,4}^{\dagger}$ contribution.

As is well known, the sign of the $q_t^{(+)}$-parameter can not be determined from frequencies but can be established from the intensities, i.e. by simulations of the ex-

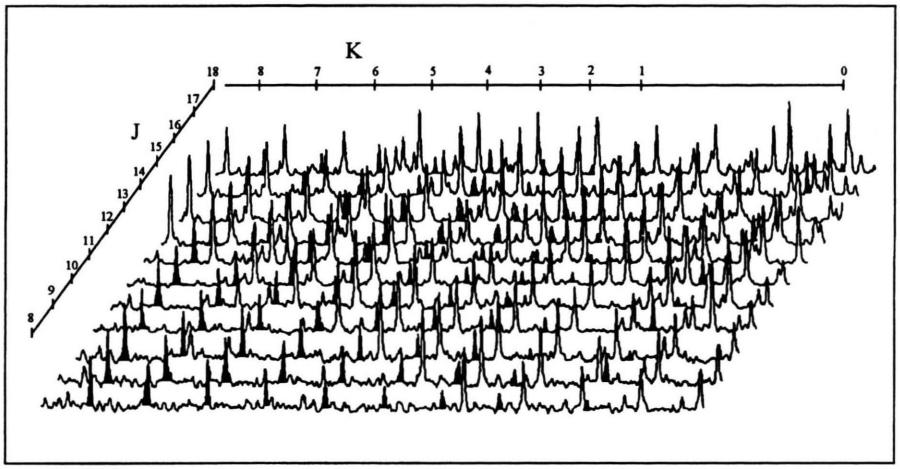

Fig. 5. Loomis-Wood plot of some $^{R}R_{K}(J)$-lines of the perpendicular band ν_9 of $^{12}C_3{}^{14}N_3H_3$. K-values from 0–8 are shown black.

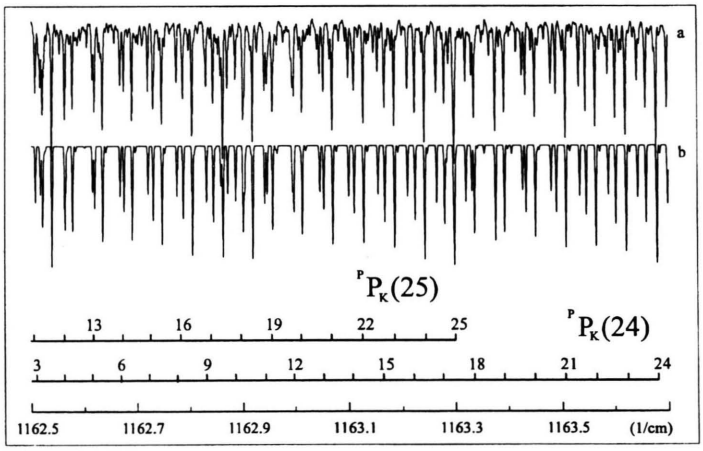

Fig. 6. Detail of the P-branches of the perpendicular band ν_9 of $^{12}C_3{}^{14}N_3H_3$. $^{P}P_{K}(24)$- and $^{P}P_{K}(25)$-lines are shown.
(a) Experimental spectrum. (b) Calculated spectrum.

perimental spectrum. We have done this for $q_7^{(+)}$ by using the program KILO [10]. As can be seen from Fig. 3, the sign of $q_7^{(+)}$ proved to be negative.

4.3. The ν_9 Fundamental Band of $^{12}C_3{}^{14}N_3H_3$, $^{13}C_3{}^{14}N_3H_3$, and $^{12}C_3{}^{15}N_3H_3$

The weak fundamental band ν_9 at 1172 cm^{-1} ($^{12}C_3{}^{14}N_3H_3$), (Fig. 4), 1153 cm^{-1} ($^{13}C_3{}^{14}N_3H_3$) and 1165 cm^{-1} ($^{12}C_3{}^{15}N_3H_3$) represents a text-book-example of a perpendicular band of a planar symmetric top molecule with respect to the separation and intensity of its subbands. Like the ν_7 band described above, the ν_9 band is free from accidental resonances at the present resolution. Contrary to the former, the ν_9 band exhibits a large negative value of ζ_9^z of about –0.73 which results in a strong $q_9^{(+)}$-resonance and the formation of intense absorption maxima for the $^{P}Q_K$-subbands with low K-values. As a further result of this resonance, the intensity of the normally very weak $^{R}R_0(J)$-transitions is enhanced, making intensity alternation and frequency shifts clearly visible (Fig. 5).

The P- and R-branches of the ν_9 band exhibit a "pseudo parallel structure", i.e. the subbands form clusters of lines with the same J-value. Contrary to the parallel band case, the transitions with the highest intensity are here the last lines $^{\Delta K}\Delta K_K(K)$ (Fig. 6).

The distance of lines within one J-cluster remains remarkably constant over the complete frequency area,

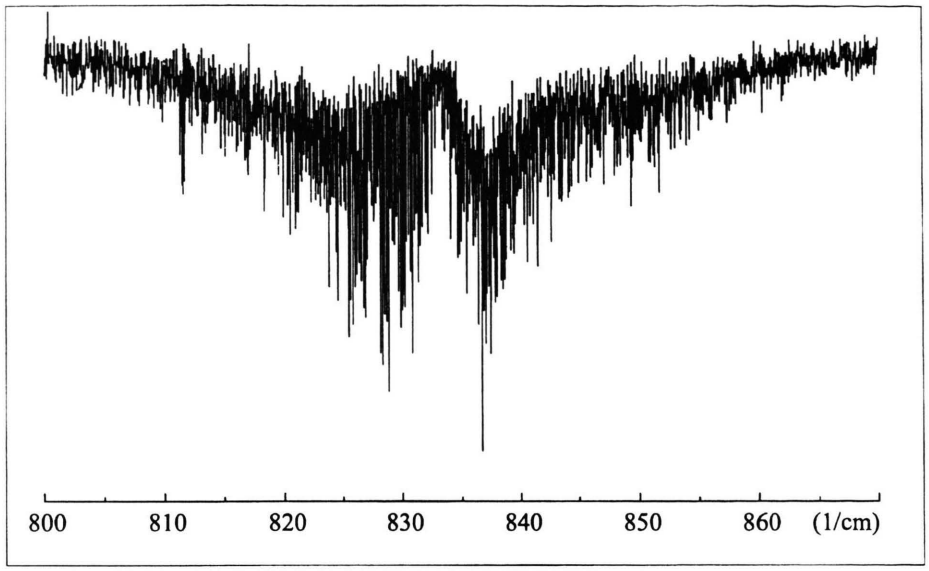

Fig. 7. The difference band $\nu_9 - \nu_{14}$ of $^{12}C_3{}^{14}N_3H_3$ (l = 144 m, p = 1.1 mbar).

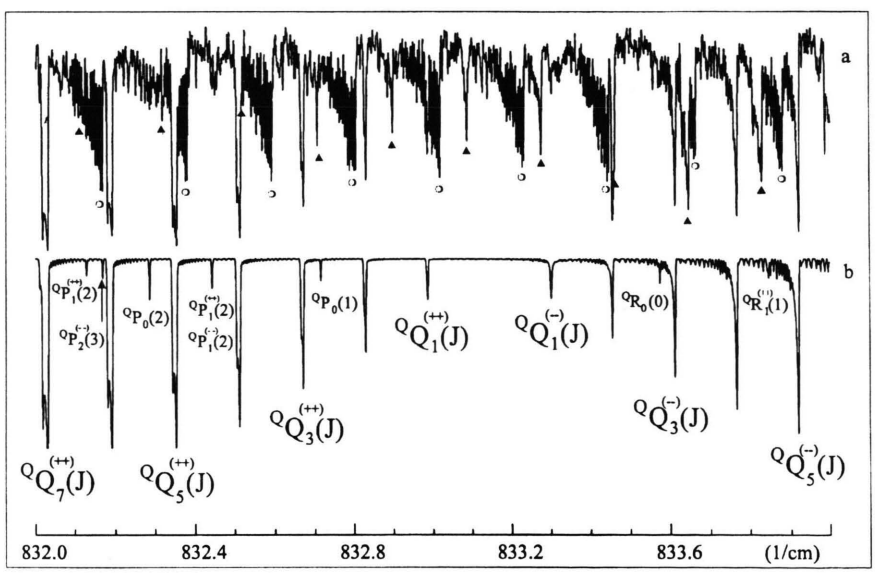

Fig. 8. Part of the central Q-branches of the difference band $\nu_9 - \nu_{14}$ of $^{12}C_3{}^{14}N_3H_3$ between 832.0 and 834.0 cm^{-1}. The observed spectrum is obscured by transitions of the hot bands $(\nu_9 + \nu_{14})^{\pm 2} - 2\nu_{14}{}^{\pm 2}$ (○) and $(\nu_9 + \nu_{14})^{0} - 2\nu_{14}{}^{0}$ (▲).
(a) Experimental spectrum (l = 144 m, p = 2.4 mbar). (b) Calculated spectrum.

leading to a very well structured spectrum showing only few line blendings.

Using GSCD's it became possible to assign 4500 lines with $-75 \le \Delta KK \le 79$ and $-80 \le \Delta KJ \le 79$ of $^{12}C_3{}^{14}N_3H_3$, 5238 lines with $-70 \le \Delta KK \le 71$ and $-74 \le \Delta KJ \le 72$ of $^{13}C_3{}^{14}N_3H_3$, and 4269 transitions with $-66 \le \Delta KK \le 63$ and $-66 \le \Delta KJ \le 64$ of $^{12}C_3{}^{15}N_3H_3$. These have been subjected to the iterative program MILLI, taking into account the essential $q_9^{(+)}$-resonance according to (3). The simulation of the $^{R}Q_0(J)$ and $^{R}R_0(J)$ subbands proves $q_9^{(+)}$ to have a positive sign.

Table 5. Molecular constants [cm^{-1}] of the ν_9 band of triazine isotopomers. (Numbers in parentheses are one standard deviation in units of the last significant digit).

	$^{12}C_3{}^{14}N_3H_3$	$^{13}C_3{}^{14}N_3H_3$	$^{12}C_3{}^{15}N_3H_3$
ν_0	1172.6397754(82)	1152.8595520(69)	1165.454628(11)
$C'' - C'$	$1.61411(19) \cdot 10^{-4}$	$1.525209(93) \cdot 10^{-4}$	$1.57197(18) \cdot 10^{-4}$
$B'' - B'$	$1.43579(18) \cdot 10^{-4}$	$1.530245(90) \cdot 10^{-4}$	$1.48024(16) \cdot 10^{-4}$
$(C\zeta)'$	$-7.847199(22) \cdot 10^{-2}$	$-7.739895(15) \cdot 10^{-2}$	$-7.953730(22) \cdot 10^{-2}$
$D_J'' - D_J'$	$-2.024(98) \cdot 10^{-10}$	$-4.400(19) \cdot 10^{-10}$	$-1.576(46) \cdot 10^{-10}$
$D_{JK}'' - D_{JK}'$	$5.73(24) \cdot 10^{-10}$	$1.3528(42) \cdot 10^{-9}$	$6.73(11) \cdot 10^{-10}$
$D_K'' - D_K'$	$-2.00(17) \cdot 10^{-10}$	$-7.183(36) \cdot 10^{-10}$	$-3.681(79) \cdot 10^{-10}$
η^J	$1.846(48) \cdot 10^{-8}$	$1.462(12) \cdot 10^{-8}$	$7.74(25) \cdot 10^{-9}$
η^K	$-6.629(49) \cdot 10^{-8}$	$6.091(14) \cdot 10^{-8}$	$-4.920(27) \cdot 10^{-8}$
$H_J'' - H_J'$	$-6.1(15) \cdot 10^{-15}$		
$H_{JK}'' - H_{JK}'$	$1.67(56) \cdot 10^{-14}$		
$H_{KJ}'' - H_{KJ}'$	$-2.33(72) \cdot 10^{-14}$		
$H_K'' - H_K'$	$1.48(38) \cdot 10^{-14}$		
η^{JJ}	$-2.0(11) \cdot 10^{-13}$		
η^{JK}	$-1.13(23) \cdot 10^{-12}$		
η^{KK}	$9.9(17) \cdot 10^{-13}$		
$q_9^{(+)}$	$4.84267(40) \cdot 10^{-4}$	$4.77391(22) \cdot 10^{-4}$	$4.57977(81) \cdot 10^{-4}$
$q_9^{(+)J}$	$-6.74(25) \cdot 10^{-10}$	$-5.26(13) \cdot 10^{-10}$	$-2.46(60) \cdot 10^{-10}$
$q_9^{(+)K}$	$-1.87(37) \cdot 10^{-14}$	$1.28(17) \cdot 10^{-14}$	$4.0(11) \cdot 10^{-14}$
σ	$178 \cdot 10^{-6}$	$199 \cdot 10^{-6}$	$261 \cdot 10^{-6}$
number of lines	4500	5238	4269

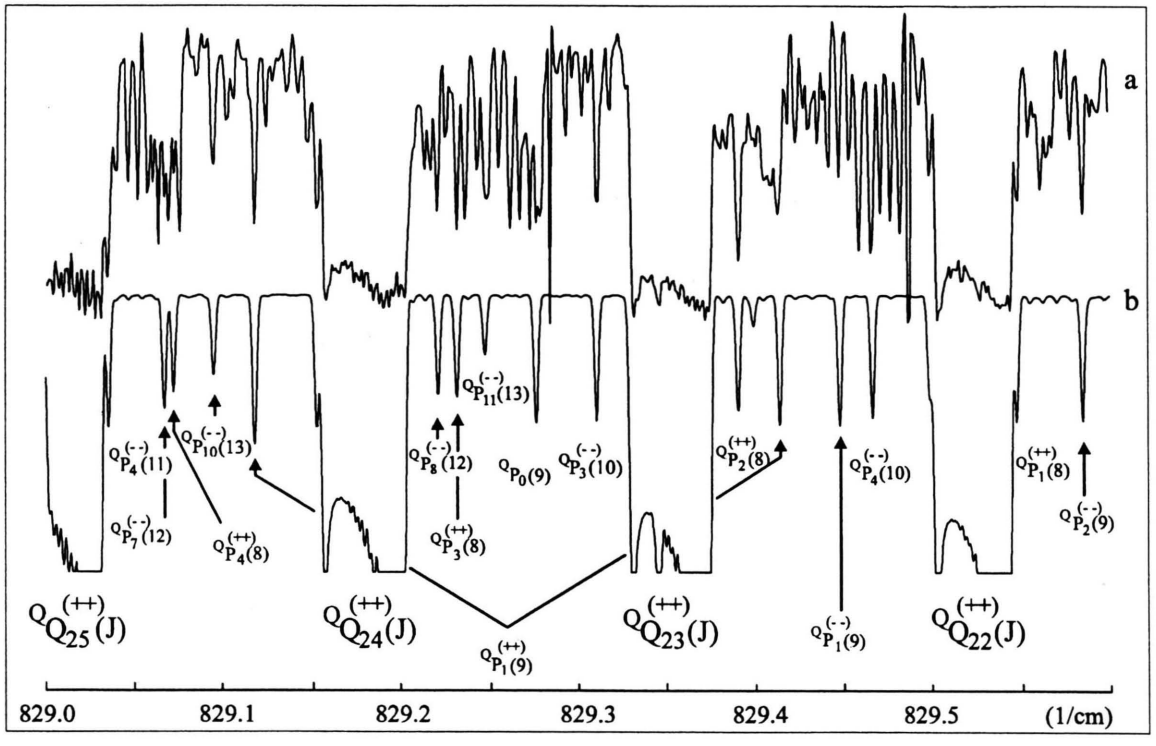

Fig. 9. Detail of the P-branches of the difference band $\nu_9 - \nu_{14}$ of $^{12}C_3{}^{14}N_3H_3$ between 829.0 and 829.6 cm^{-1}. The $^{Q}P_1^{(++)}(J)$-transitions exhibit a strong A_1/A_2-splitting. The spectrum is obscured by hot band transitions.
(a) Experimental spectrum (l = 144 m, p = 2.4 mbar). (b) Calculated spectrum.

The lines used as input data are all unblended and, therefore, equally weighted. The results are set out in Table 3. In the case of $^{13}C_3{}^{14}N_3H_3$ and $^{12}C_3{}^{15}N_3H_3$ the quality of the spectra allowed only a fit up to the η's.

4.4. The Difference Band $\nu_9 - \nu_{14}$ of $^{12}C_3{}^{14}N_3H_3$

In [2] we had reported on a method to determine the molecular constants of the lowest fundamental band ν_{14} which is IR-inactive. At that time, the quality of the parameters established could not be verified because of the lack of an experimental spectrum of the ν_{14} band.

In the meantime, this verification became possible by the analysis of the difference band $\nu_9 - \nu_{14}$ of $^{12}C_3{}^{14}N_3H_3$. This difference band at 833 cm^{-1} is very weak and can only be observed with a White cell (Figure 7). As can be seen from the Fig. 8 and 9, the spectrum of the $\nu_9 - \nu_{14}$ difference band is obscured by the hot bands $(\nu_9 + \nu_{14})^{\pm 2} - 2\nu_{14}{}^{\pm 2}$ and $(\nu_9 + \nu_{14})^{0} - 2\nu_{14}{}^{0}$, respectively. Nevertheless, the "cold" lines, i.e. the lines having $\boldsymbol{v}_{14} = 1$ as lower state, are clearly discernible.

The $\nu_9 - \nu_{14}$ difference band is characterized by a PAPE-structure (parallel band with perpendicular structure) [11]. As a result of the large difference of $(C\zeta)_{14} - (C\zeta)_9$ of $7.845 \cdot 10^{-2}$ cm^{-1}, all transitions $J'' \rightarrow J'$ split into the two components $(+l) \rightarrow (+l)$ $((++))$ and $(-l) \rightarrow (-l)$ $((--))$, which are spread out over the whole spectrum. In the present case, $^{Q}QK^{(++)}(J)$-transitions are shifted to lower wavenumbers, while $^{Q}QK^{(--)}(J)$ are shifted to higher wavenumbers (Figure 8). The difference of the $q_t^{(+)}$-parameters of the two niveaus involved results in a strong A_1/A_2-splitting of levels with $kl = +1$, as can be seen from Figure 9. Using the molecular constants of the lower state $\boldsymbol{v}_{14} = 1$ [2] and of the upper state $\boldsymbol{v}_9 = 1$ (Table 5), about 3600 transitions of the difference band $\nu_9 - \nu_{14}$ could be assigned and fitted with a standard deviation $\sigma = 382 \cdot 10^6$ cm^{-1}. The fitted parameters of the $\nu_9 - \nu_{14}$ difference band are not given here because they do not deviate significantly from the corresponding differences of parameters of $\boldsymbol{v}_9 = 1$ and $\boldsymbol{v}_{14} = 1$, respectively.

As the Figs. 8 and 9 show, the spectrum of the $\nu_9 - \nu_{14}$ difference band is nicely reproduced by these parameters, proving thereby the quality of the molecular constants of the ν_{14} fundamental band.

5. Conclusion

In the present study the perpendicular bands ν_7 and ν_9 of the isotopomers $^{12}C_3{}^{14}N_3H_3$, $^{13}C_3{}^{14}N_3H_3$ and $^{12}C_3{}^{15}N_3H_3$ have been analyzed and the molecular constants of the states $\boldsymbol{v}_7 = 1$ and $\boldsymbol{v}_9 = 1$ are given. By combining the molecular constants of $\boldsymbol{v}_9 = 1$ and of $\boldsymbol{v}_{14} = 1$ [2], the analysis of the weak difference band $\nu_9 - \nu_{14}$ of $^{12}C_3{}^{14}N_3H_3$ was possible, thus verifying the constants of the IR-inactive band ν_{14}.

The analysis of the other IR-active perpendicular bands of the triazines considered and of all IR-active fundamental of the isotopomers $^{13}C_3{}^{14}N_3H_3$ and $^{12}C_3{}^{15}N_3H_3$ will be the subject of some forthcoming papers.

Acknowledgements

We are grateful to Dr. Stefan Klee and Georg Mellau (University of Gießen) and to Dr. Risto Paso, Matti Koivusaari, Jyrki Schroderus, and Seppo Alanko (University of Oulu) for recording the spectra. One of us (W.B) expresses his gratitude to the Landesgraduiertenstiftung for support of this work. The support of the Deutsche Forschungsgemeinschaft in making available the FT-IR spectrometer at Gießen is gratefully acknowledged.

[1] W. Bodenmüller, A. Ruoff, and L. Manceron, Z. Naturforsch. **47a**, 1197 (1992).
[2] W. Bodenmüller and A. Ruoff, J. Mol. Spectrosc. **173**, 205 (1995).
[3] W. Bodenmüller, M. Pfeffer, B. Macht, R. Ruber, and A. Ruoff, Z. Naturforsch **53a**, 1 (1998).
[4] C. A. Morrison, B. A. Smart, D. W. H. Rankin, and H. E. Robertson, M. Pfeffer, W. Bodenmüller, R. Ruber, B. Macht, A. Ruoff, and V. Typke, J. Phys. Chem. A **101**, 10029 (1997).
[5] G. Guelachvili and K. Narahari Rao, Handbook on Infrared Standards. Academic Press Inc., London 1986.
[6] J. K. G. Watson in: J. R. Durig (ed.), Vibrational Spectra and Structure, Vol. 6, Elsevier, New York 1977.
[7] J. Pliva, J. Mol. Spectrosc. **120**, 5 (1985).
[8] G. J. Cartwright and J. M. Mills, J. Mol. Spectrosc. **34**, 415 (1970).
[9] S. J. Daunt and H. F. Shurvell, J. Mol. Spectrosc. **62**, 373 (1976).
[10] G. Graner, private communication.
[11] G. Graner, J. Mol. Spectrosc. **161**, 58 (1993).